ES Food and Agroforestry
DOI: https://dx.doi.org/10.30919/faf1746

Green Synthesis and Characterization of Zinc Oxide Nanoparticles using *Alpinia Officinarum* Rhizome Extract for Antimicrobial, Antioxidant and Anti-biofilm Applications

Nishkala Krishnamoorthy[1], Suganya Kannan[2] and Ragupathy Dhanusuraman[1,3,*]

Abstract

Zinc oxide (ZnO) nanoparticles (NPs) have emerged as a significant area of research due to their distinctive physicochemical and biological properties. In this study, an eco-friendly and cost-effective synthesis of ZnO NPs was achieved using *Alpinia officinarum (A. officinarum)* rhizome extract in conjunction with Zinc nitrate hexahydrate as a precursor. The structural and morphological properties of the synthesized ZnO NPs were characterized using X-ray diffraction (XRD), Fourier-transform infrared spectroscopy (FTIR), and transmission electron microscopy (TEM). FTIR analysis confirmed the presence of functional groups associated with the phytochemicals involved in the synthesis process. Crystalline structure and particle size were validated through XRD and TEM analyses. The antimicrobial potential of the ZnO NPs was evaluated against *Pseudomonas aeruginosa* ATCC 25619, methicillin-resistant *Staphylococcus aureus* (MRSA) ATCC 43300, and *Candida albicans* ATCC 10231. Additionally, antibiofilm assays were conducted against the same microbial strains. The ZnO NPs demonstrated significant antimicrobial and antibiofilm efficacy. These findings suggest that biosynthesized ZnO NPs possess promising potential for application in biomedical coatings, pharmaceuticals, and cosmetic formulations.

Keywords: Alphinia officinarum; ZnO nanoparticles; Methicillin-resistant *Staphylococcus aureus*; *Pseudomonas aeruginosa.*
Received: 08 January 2025; Revised: 20 June 2025; Accepted: 26 September 2025
Article type: Research article.

1. Introduction

Nanotechnology is an emerging area that emphasizes creating materials at the nanoscale (1-100 nm). It provides vast possibilities in numerous fields by developing innovative nanomaterials with distinct properties that depend on their size. Nanotechnology advances optics, energy generation, enables targeted drug delivery in medicine, and supports environmental science applications.[1] Since the emergence of nanotechnology, scientists have created a range of nanoscale devices employing diverse synthesis methods, such as physical, chemical, and eco-friendly techniques. Among these, green synthesis has appeared as a novel and adaptable approach.[2] Green synthesis has emerged as a sustainable and economical alternative to conventional nanoparticle production methods. It reduces the use of harmful chemicals and supports the development of nanomaterials with specific properties and high biocompatibility.[3] This approach utilizes biological entities such as plant extracts, bacteria, fungi, and algae as natural reducing and capping agents, enabling environmentally benign synthesis with controlled morphology.[4] This method has facilitated the fabrication of a wide range of nanomaterials, such as carbon nanostructures, metal-organic frameworks,[5] and particularly metal oxide nanoparticles, which are increasingly utilized in environmental remediation, biomedical applications, and energy-related technologies.[6–8]

Among various metal oxides, ZnO NPs have attracted considerable interest among various metal oxides, owing to their versatile functionalities and unique physicochemical characteristics.[9] These include a wide bandgap, vigorous photocatalytic activity, high UV absorption capacity, and excellent photostability, enabling their use in electronics, optoelectronics, sensors, and solar energy conversion devices.[10] Compared to conventional physical and chemical synthesis techniques such as sol-gel processing, hydrothermal methods, and electrodeposition, the green synthesis of ZnO

[1]*Nano Electrochemistry Lab (NEL), Department of Chemistry, National Institute of Technology Karaikal, Puducherry, 609609, India*
[2]*Central Research Laboratory for Biomedical Research, Vinayaka Mission's Medical College and Hospital, Vinayaka Mission's Research Foundation (Deemed to be University), Karaikal, Puducherry, 609609, India*

NPs offers a cost-effective, simple, and more environmentally sustainable alternative. This method converts Zinc precursors into ZnO NPs using biologically active compounds, such as flavonoids, terpenoids, and phenolics, from plant extracts, which act as natural reductants and stabilizing agents.[11]

ZnO NPs have a range of technological and biomedical applications, including drug delivery, bioimaging, wound healing, cancer therapy, and antimicrobial treatments. Their therapeutic efficacy is primarily due to their ability to generate reactive oxygen species (ROS), penetrate cellular membranes, and selectively induce cytotoxicity in microbial and cancer cells.[12-13] In addition to the biomedical uses, ZnO NPs also have potential in agroforestry and environmental sustainability, where they increase crop productivity, enhance soil quality, and support sustainable forest management.[14] ZnO NPs are generally regarded as safe for biomedical use, which has encouraged their incorporation into healthcare products. They are extensively used in cosmetics, especially as UV filters in sunscreen formulations, and are also applied as antimicrobial coatings on medical tools and devices.[15-16] These applications derive from ZnO NP's unique electronic, optical, and chemical properties at the nanoscale.[17]

Despite significant progress, concerns over long-term biocompatibility, dose-dependent cytotoxicity, and the lack of standardized synthesis protocols have limited the biomedical application of ZnO NPs. The molecular and cellular interactions of ZnO NPs remain insufficiently understood.[18] Therefore, comprehensive studies are essential to optimize their synthesis, characterize their properties, and evaluate their biomedicine; this review proposes that green-synthesized ZnO NPs possess the enhanced potential for biomedical applications, particularly in antimicrobial and anticancer treatments, owing to their improved biocompatibility, functional adaptability, and ecological sustainability.[19] This study presents a comprehensive review of green synthesis approaches, physicochemical characteristics, and proposed formation mechanisms of ZnO NPs, emphasizing their emerging applications in the biomedical field, to evaluate this hypothesis.[20-21] This method creates ZnO NPs from zinc precursors by utilizing physiologically active substances present in plant extracts, such as flavonoids, terpenoids, and phenolics, which function as organic reducing and stabilizing agents.[22-23]

This study explores the biomedical applications of ZnO NPs synthesized using *A. officinarum* rhizome extract. Although green synthesis of metal oxide nanoparticles has been extensively explored, the utilization of *A. officinarum* for the biosynthesis of ZnO NPs represents a novel approach that, to the best of our knowledge, has not yet been reported in the existing scientific literature.. This study presents a novel plant-mediated approach employing *A. officinarum* rhizome, known for its abundance of phenolic and flavonoid compounds, which contribute significantly to nanoparticle formation and stabilization. In contrast to prior investigations that often examine a single biological activity, the current work offers a comprehensive evaluation of the synthesized ZnO NPs, including their antimicrobial, antioxidant, and anti-biofilm properties. This integrated analysis enhances the understanding of the potential biomedical applications of ZnO NPs. Furthermore, the synthesis approach is environmentally nontoxic, economically viable, and devoid of hazardous reducing or stabilizing agents, thereby adhering to the principles of green chemistry.

2. Materials and methods

2.1 Chemicals

Zinc nitrate hexahydrate ($Zn(NO_3)_2 \cdot 6H_2O$) was procured from Sisco Research Laboratory (India). Muller-Hinton agar, nutrient broth, gentamicin antibiotic solution, and amphotericin B antimycotic solution were obtained from HiMedia Laboratories (India). The microbial strains *Pseudomonas aeruginosa* (ATCC 25619), methicillin-resistant *Staphylococcus aureus* (MRSA, ATCC 43300), and *Candida albicans* (ATCC 10231) were acquired from the Microbial Type Culture Collection (MTCC), Chandigarh, India. All experimental procedures were carried out using deionized water.

2.2 Preparation of *A. officinarum* leaves extract

A. officinarum is a perennial herb of the family Zingiberaceae. It is widely cultivated across various regions of Southeast Asia and the Indian subcontinent due to its medicinal and economic significance. The dried rhizomes of *A. officinarum* were sourced from a certified herbal supplier in Karaikal, Puducherry, India. The rhizomes were initially rinsed three times—first with tap water and subsequently with deionized water—to eliminate surface impurities. The cleaned samples were then shade-dried for a period of 20 days. Once dried, the rhizomes were ground into a fine powder using a mortar and pestle.

To prepare the extract, 5 grams of powdered rhizome were mixed with 100 mL of distilled water in a conical flask. The mixture was heated at 60 °C for 24 hours. After cooling to room temperature, the extract was filtered through Whatman No. 1 filter paper. The resulting filtrate was stored at 4 °C and used in subsequent nanoparticle synthesis procedures.

2.3 Synthesis of *A. officinarum* rhizome extract facilitated ZnO-NPs

A 50 mL aliquot of *A. officinarum* rhizome extract was heated to 60–70 °C, followed by the addition of a 0.1 M zinc nitrate hexahydrate [$Zn(NO_3)_2 \cdot 6H_2O$] solution (in a 1:1 v/v ratio with the extract) under continuous stirring. The mixture was maintained at this temperature to facilitate the gradual

[3]*Nano Electrochemistry Laboratory (NEL), Central Instrumentation Facility (CIF), School of Physical, Chemical and Applied Sciences, Pondicherry University, Karaikal, Puducherry, 605014, India*
**Email:* ragu@pondiuni.ac.in, ragu.nitpy@gmail.com
(Ragupathy Dhanusuraman)

reduction of Zn^{2+} ions, resulting in the formation of a brownish-white $Zn(OH)_2$ paste. The paste was then dried in a hot-air oven at 70 °C for 2 hours to remove residual moisture. The dried mass was calcinated in a muffle furnace at 500 °C for 2 hours under a constant flow of oxygen to obtain ZnO NPs in powder form. The final product was ground using a mortar and pestle and stored in an airtight container for further characterization.

2.4 Characteristic analysis for nanoparticles

X-ray diffraction (XRD) analysis was performed using a Panalytical X'Pert PRO diffractometer equipped with a Cu-Kα radiation source (λ = 1.54056 Å). The diffraction patterns were recorded over a 2θ range of 20° to 80°, with a step size of 0.02° and a scan rate of 2°/min, to evaluate the phase purity, crystallinity, and average crystallite size of the synthesized ZnO NPs. Fourier-transform infrared spectroscopy (FTIR) was employed to identify the functional groups present in the rhizome extract of *A. officinarum* and its role in the synthesis of ZnO NPs. The analysis was carried out in the spectral range of 4000–400 cm^{-1} using the KBr pellet method on a PerkinElmer Spectrum RX1 spectrometer. HR-TEM was utilized to determine the morphology and particle size of the ZnO NPs. The analysis was conducted using a JEOL 4000 instrument operated at an accelerating voltage of 400 kV.

2.5 Antimicrobial activity determination and minimum inhibitory concentration (MIC) determination

The antibacterial and antifungal efficacy of the biosynthesized ZnO NPs was evaluated against Pseudomonas aeruginosa (ATCC 25619), methicillin-resistant Staphylococcus aureus (MRSA, ATCC 43300), and Candida albicans (ATCC 10231), representing Gram-negative bacteria, Gram-positive bacteria, and yeast, respectively. The agar well diffusion method was employed using Mueller-Hinton agar (MHA) for bacterial strains and Sabouraud dextrose agar (SDA) for C. albicans. Nutrient broth was used to culture the test organisms. Mueller-Hinton agar was prepared by dissolving 2.8–3.0 g in deionized water, followed by autoclaving at 121°C for 15 minutes under 15 psi pressure. After cooling, 20 mL of the molten medium was poured into sterile 100 mm Petri dishes and allowed to solidify. A standardized microbial suspension (OD600 ≈ 0.5) equivalent to 1 × 10^5 CFU/mL was prepared and uniformly spread over the agar surface. Wells were punched aseptically and loaded with 50, 100, 200, and 500 µg/mL of ZnO NP suspensions. Gentamicin was used as the positive control. Plates were incubated at 37°C for 24 hours, and zones of inhibition were measured in millimeters. All experiments were performed in triplicate for statistical consistency.

The minimum inhibitory concentration (MIC) of ZnO NPs was determined by broth microdilution in Mueller-Hinton broth (MHB). A series of twofold serial dilutions of ZnO NPs (ranging from 1 to 1000 µg/mL) were prepared in sterile 96-well microtiter plates. Exponentially growing cultures were diluted 1:10 in MHB to achieve an inoculum density of approximately 1 × 10^5 CFU/mL per well. After inoculation, plates were incubated at 37°C for 16–24 hours. Post-incubation, bacterial growth was assessed spectrophotometrically by measuring absorbance at 600 nm using a SpectraMax M3 microplate reader (Molecular Devices, USA). MIC was defined as the lowest concentration of ZnO NPs that inhibited visible microbial growth.

2.6 Biofilm biomass analysis

The inhibitory effect of ZnO NPs on biofilm formation was evaluated using the microtiter plate assay method as described previously.[24] Briefly, Candida albicans cells were inoculated into a 96-well microtiter plate and incubated at room temperature for 18 hours in both the presence and absence of ZnO NPs. Following incubation, non-adherent planktonic cells were carefully removed, and the wells were gently rinsed with distilled water. Surface-adhered biofilm cells were stained with 0.4% crystal violet solution for 10 minutes. Excess stain was removed by washing with distilled water, and the plates were allowed to air dry. Subsequently, 1 mL of 20% glacial acetic acid was added to each well to solubilize the bound crystal violet. The absorbance of the resulting solution was measured at 570 nm using a UV-visible spectrophotometer to quantify biofilm biomass.

For microscopic evaluation, biofilms were developed on sterile glass slides (1 cm × 1 cm) placed in culture media with and without ZnO NPs. The slides were incubated for 24 hours at 37 °C in triplicate. After incubation, excess media and loosely attached cells were removed by rinsing, and the slides were air-dried. After air-drying, the prepared slides were observed under a Nikon Eclipse 80i microscope (Nikon Instruments, USA) at 400× magnification for light microscopy analysis. To facilitate confocal laser scanning microscopy (CLSM), the biofilms were stained in the dark with 0.1% acridine orange for two minutes. Following staining, the slides were gently rinsed with sterile distilled water, allowed to dry, and subsequently examined under CLSM. The structural organization of the biofilms was then evaluated using COMSTAT image analysis software.[25]

2.7 Estimation of in vitro antioxidant property

2.7.1 DPPH radical scavenging activity

The free radical scavenging activity of ZnO NPs was evaluated using the method described.[26] Briefly, 0.1 mL of ZnO NP suspension was diluted with 1.5 mL of methanol. Subsequently, 1.5 mL of this solution was mixed with 0.2 mM 2,2-diphenyl-1-picrylhydrazyl (DPPH) radical solution. The mixture was thoroughly homogenized and incubated in the dark at room temperature for 20 minutes. The absorbance was recorded at 517 nm using a UV-visible spectrophotometer. Rutin was employed as a positive control in the assay.

3. Results and discussion

3.1 Synthesis Mechanism of ZnO NPs using *A. officinarum* rhizome extract

In the present study, ZnO NPs were synthesized via a green approach using A officinarum rhizome extract. The bioactive compounds within the extract served dual roles as both reducing and stabilizing agents during nanoparticle formation. The root extract is known to contain various phytochemicals, notably 6-gingerol and its derivative 6-shogaol as major constituents.[27] Additionally, the presence of flavonoids such as galangin, kaempferol, and quercetin further enhances its bio-reducing capacity.[28] Based on the chemical composition of the extract, a plausible mechanism for the biosynthesis of ZnO NPs is proposed below:

3.1.1 Dissolution of zinc nitrate hexahydrate

Zinc nitrate hexahydrate ($Zn(NO_3)_2 \cdot 6H_2O$) readily dissolves in the extract, dissociating into zinc ions (Zn^{2+}), nitrate ions (NO_3^-), and water molecules, forming a clear aqueous solution Eq. (1)

$$Zn(NO_3)_2.\ 6H_2O \rightarrow Zn^{2+} + 2NO_3^- + 6\ H_2O \quad (1)$$

3.1.2 Coordination and reduction by phytochemicals

The Zn^{2+} ions released into solution subsequently interact with various phytochemicals present in the *A. officinarum* rhizome extract. Bioactive compounds like 6-gingerol, 6-shogaol, kaempferol, and quercetin—known for their abundance of hydroxyl and phenolic groups—interact with Zn^{2+} ions through both ionic interactions and hydrogen bonding. These compounds act as natural reducing agents, facilitating the reduction of Zn^{2+} and resulting in the generation of zinc hydroxide ($Zn(OH)_2$) . In addition to their reductive function, these phytochemicals serve as capping agents, preventing agglomeration and assisting in the stabilization and shape control of the forming nanoparticles.[29]

3.1.3 Development of ZnO NPs

The intermediate compound, zinc hydroxide ($Zn(OH)_2$), is subsequently exposed to heat treatment at 500 °C. This calcination process leads to the decomposition of $Zn(OH)_2$ into ZnO, accompanied by the release of water molecules.[30] The thermal conversion results in the formation of stable, crystalline ZnO NPs, as illustrated in Fig. 1 (a) and (b).

3.2 X-ray Diffraction analysis

The crystalline structure of the ZnO NPs synthesized using *A. officinarum* rhizome extract was characterized by X-ray diffraction (XRD) analysis. The diffraction pattern was recorded over a 2θ range of 10° to 80°, revealing distinct and sharp peaks indicative of high crystallinity and phase purity. The observed diffraction peaks appeared at 2θ values of approximately 31.75°, 34.40°, 36.25°, 47.63°, 56.61°, 62.89°, 66.49°, 67.99°, and 69.14°, corresponding to the (100), (002), (101), (102), (110), (103), (200), (112), and (201) crystallographic planes, respectively. These values are in good agreement with the standard data from the Joint Committee on Powder Diffraction Standards (JCPDS card no. 89-1397), confirming the formation of a hexagonal wurtzite structure, as

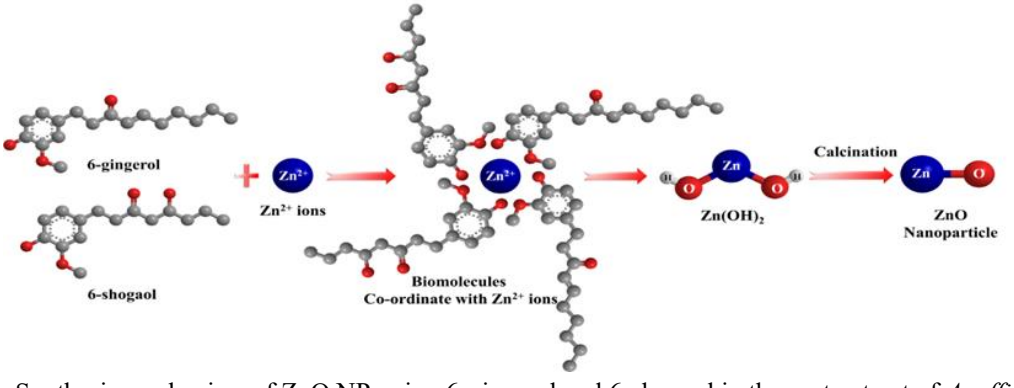


Fig. 1(a): Synthesis mechanism of ZnO NPsusing 6-gingerol and 6-shogaol in the root extract of *A. officinarum.*

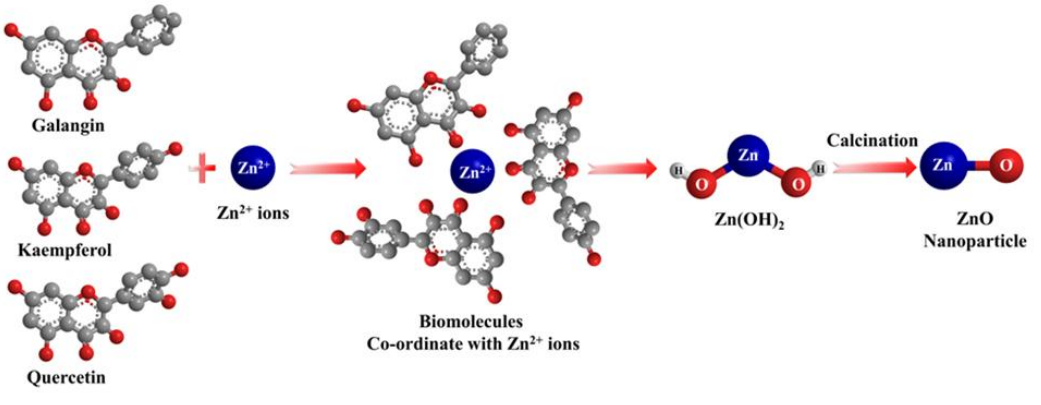


Fig. 1(b): Synthesis mechanism of ZnO NPs using shogaol, kaempferol and quercetin in the root extract of *A. officinarum.*

illustrated in Fig. 2.[31]

$$D = \frac{K\lambda}{\beta \cos\theta} \quad (2)$$

The average crystallite size of the ZnO NPs was estimated using the Debye–Scherrer equation (Eq. 2), based on the most intense diffraction peak at 2θ = 36.25°, corresponding to the (101) plane. The calculated crystallite size was approximately 20 nm, indicating the successful formation of nanoscale particles with a well-defined hexagonal phase.

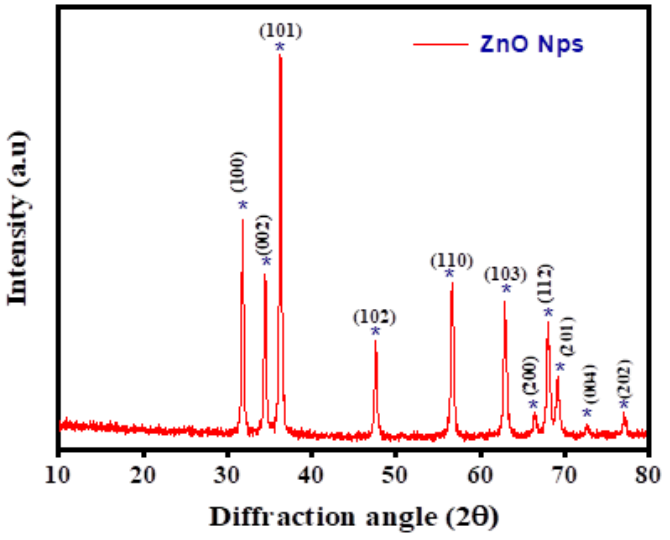


Fig. 2: XRD pattern of ZnO NPs.

3.3 FT-IR studies

Fourier Transform Infrared (FT-IR) spectroscopy was employed to identify the functional groups involved in the synthesis of ZnO nanoparticles (ZnONPs) using *A. officinarum* rhizome extract. The FT-IR spectrum of the plant extract (Fig. 3a) exhibited prominent absorption bands at 3430 cm^{-1} and 1636 cm^{-1}, corresponding to O–H stretching vibrations, indicating hydroxyl functional groups. A band around 2932 cm^{-1} was assigned to C–H stretching, while the absorption near 1446 cm^{-1} corresponded to C=O stretching, which are characteristics of flavonoid compounds. A distinct peak at 1389 cm^{-1} suggested the presence of C=N bonds, and additional bands at 1113 cm^{-1} and 1040 cm^{-1} were attributed to C–O and C–C stretching vibrations, respectively. Furthermore, a peak at 1121 cm^{-1} indicated C–C stretching, typically observed in terpenoids.[32]

The FT-IR spectrum of ZnONPs synthesized using the rhizome extract (Fig. 3b) displayed a broad peak at 3436 cm^{-1}, assigned to O–H stretching vibrations, likely due to moisture adsorption from the environment.[32] A sharp peak at 869 cm^{-1}, along with a strong absorption at 431 cm^{-1}, confirmed the presence of Zn–O stretching vibrations. Additionally, bands observed between 600 and 300 cm^{-1} are characteristic of metal–oxygen (M–O) bonds.[33] These findings confirm the participation of plant-derived compounds such as polyphenols, flavonoids, and terpenoids, which serve as reducing and stabilizing agents. These bioactive molecules facilitate the conversion of Zn^{2+} ions into ZnO and help in capping and stabilizing the nanoparticles during synthesis.[31]

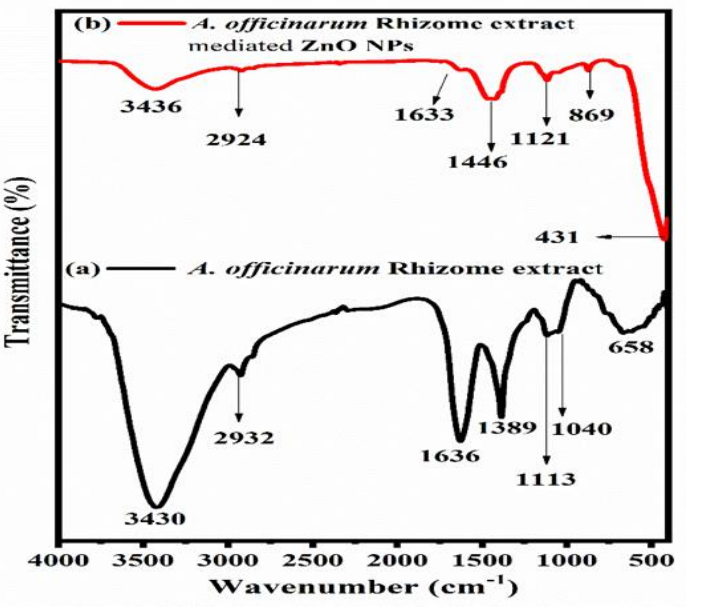


Fig. 3: (a) FTIR spectra of *A.officinarum* rhizome extract, (b) FTIR spectra of ZnO NPs.

3.4 HR-TEM with SAED pattern analysis

The crystallinity, particle size, and nanostructure of the ZnO NPs synthesized using *A. officinarum* rhizome extract were investigated using HR-TEM. The TEM images confirmed that the nanoparticles were well-dispersed and uniformly distributed without notable agglomeration (Fig. 4a and b).[36] This dispersion is attributed to the bioactive constituents present in the extract, which likely acted as natural capping and stabilizing agents during the synthesis process. Micrographs obtained at magnifications of 10 nm and 5 nm were analyzed using ImageJ software to estimate the particle size.[37] The particle size of the ZnO NPs ranged from 10 to 12 nm, with an average size of 10.12 ± 0.4 nm (Fig. 4 b). The nanoparticles exhibited a predominantly spherical morphology and a polycrystalline nature.[38,39] Furthermore, the selected area electron diffraction (SAED) pattern exhibited well-defined concentric rings indexed to (103), (110), (102), (101), (002) and (100) lattice planes planes (Fig. 4c), indicating the hexagonal wurtzite phase of ZnO NPS.[38,39]. The interplanar spacing (d-spacing) corresponding to the most intense reflection was measured to be 0.26 nm, which is consistent with the standard JCPDS card No. 89-1397.

3.5 Antimicrobial Activity determination and minimum inhibitory concentration (mic) determination.

The antimicrobial activity of biosynthesized ZnO NPs was evaluated using the Kirby–Bauer disc diffusion method against two clinically relevant bacterial strains: methicillin-resistant Staphylococcus aureus (MRSA), a gram-positive

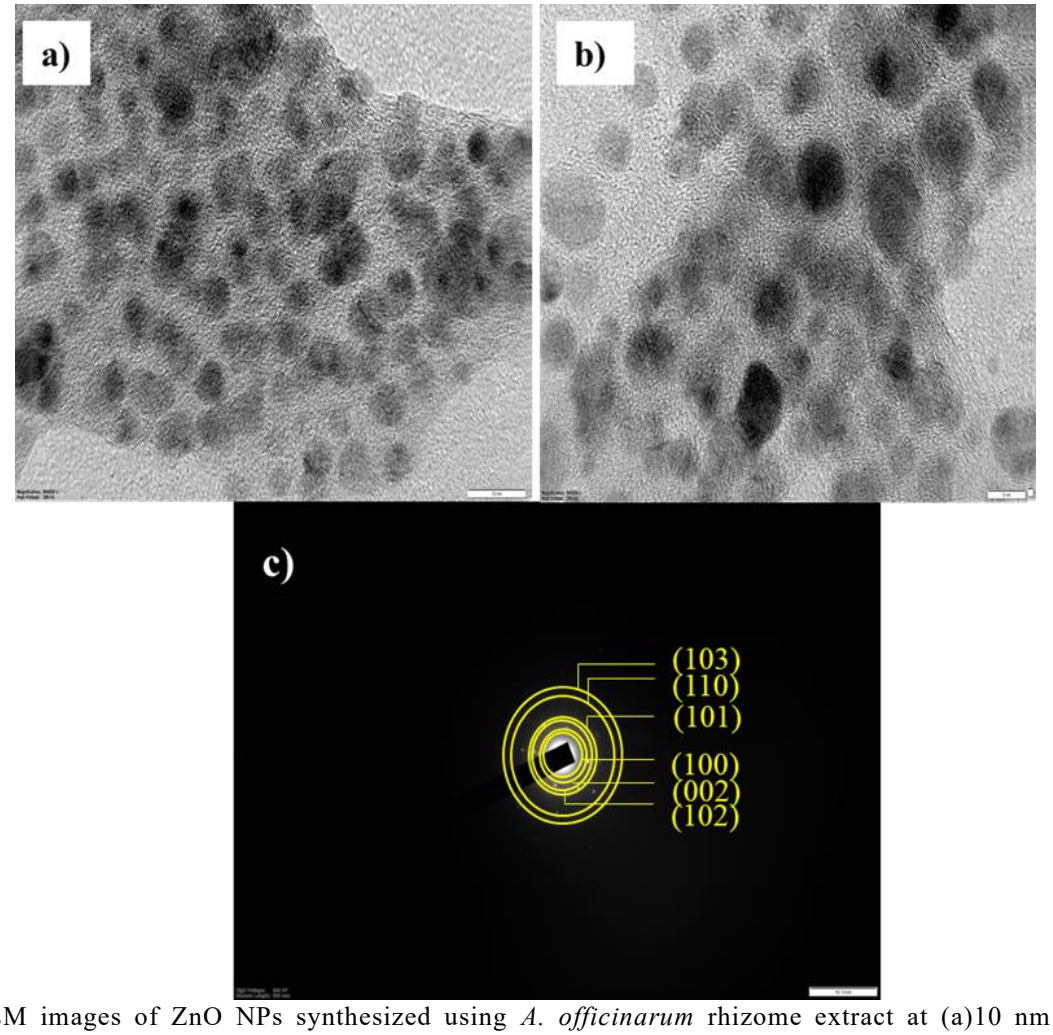


Fig. 4: HR-TEM images of ZnO NPs synthesized using *A. officinarum* rhizome extract at (a)10 nm and (b) 5 nm magnifications. (c) SAED pattern.

bacterium, and Pseudomonas aeruginosa, a gram-negative bacterium, as well as the opportunistic fungal pathogen Candida albicans.[40] Antibacterial activity was assessed at various concentrations of ZnO NPs (10, 20, 30, 40, and 50 µg/mL), and the corresponding zones of inhibition were recorded. For MRSA, the inhibition zones increased progressively with concentration, measuring 18 mm, 22 mm, 24 mm, 28 mm, and reaching 32 mm at 50 µg/mL. Similarly, P. aeruginosa exhibited strong dose-dependent inhibition, with zones measuring 20 mm, 26 mm, 34 mm, 36 mm, and peaking at 38 mm at the highest concentration. Similarly, antifungal activity against C. albicans revealed inhibition zones of 10 mm, 13 mm, 18 mm, 24 mm, and 30 mm across the same concentration gradient.[41].These findings, summarized in Table 1, demonstrate that the green-synthesized ZnO NPs possess potent and concentration-dependent antimicrobial activity against both gram-positive and gram-negative bacterial strains, as well as fungal pathogens.[42,43]

The antimicrobial mechanism of green-synthesized ZnO NPs is multifactorial and concentration-dependent. In the case of bacterial inhibition, electrostatic interactions play a critical role, wherein the positively charged Zn^{2+} ions are attracted to the negatively charged bacterial cell membranes, leading to membrane destabilization and increased permeability.[44] Furthermore, Zn^{2+} ions are known to form stable coordination complexes with amino and thiol groups present in membrane-associated proteins. These interactions can cause protein denaturation, inhibition of enzymatic activity, and disruption of vital cellular functions such as DNA replication and metabolic regulation.[45]

In addition to their antibacterial effects, ZnO NPs also exhibit antifungal activity, particularly against Candida albicans. The fungal cell wall, primarily composed of chitin and β-glucans, forms a highly ordered and hydrogen-bonded matrix that confers mechanical strength and resistance. At elevated nanoparticle concentrations, Zn^{2+} ions interfere with chitin biosynthesis and compromise the polymeric structure of the wall, resulting in weakened cell wall integrit.[46,47] Moreover, Zn^{2+} species can form coordination bonds with hydroxyl and amino functional groups within the cell wall, thereby altering its architecture. These interactions may inhibit the function of chitin synthase enzymes, such as those encoded by the CHS1 gene, disrupting septum formation and normal cell division.[48,49]

The primary antimicrobial mechanism involves the induction of oxidative stress through reactive oxygen species

Table 1: ZOI values of ZnO NPs against MRSA , Pseudomonas aureginosa, and Candida albicans.

S.No	Name of the test organism	Zone of inhibition (mm)						
		10µg/ml	20µg/ml	30µg/ml	40µg/ml	50µg/ml	10µg/ml	20µg/ml
1.	MRSA	18mm	22mm	24mm	28mm	32mm	18mm	22mm
2.	*Pseudomonas aeruginosa*	20mm	26mm	34mm	36mm	38mm	20mm	26mm
3.	*Candida albicans*	10mm	13mm	18mm	24mm	30mm	10mm	13mm

(ROS) generation. Upon exposure to light or appropriate energy input, ZnO NPs facilitate the excitation of electrons from the valence band to the conduction band, leaving behind holes (h^+) (Eq. 3). These valence band holes oxidize surface-adsorbed water molecules, generating hydroxyl radicals (OH) and protons (H^+) (Eq. 4), while conduction band electrons reduce molecular oxygen (O_2) to yield superoxide radicals (O_2^-) (Eq. 5). Through successive reactions with protons and electrons, these radicals can further form hydrogen peroxide (H_2O_2) (Eq. 6), which can subsequently decompose into additional hydroxyl radicals (•OH) (Eq. 7). Unlike other negatively charged ROS, H_2O_2 can traverse the microbial cell envelope due to its neutral or slightly positive charge, leading to oxidative damage of intracellular components, including lipids, proteins, and nucleic acids. This oxidative stress results in membrane dysfunction, impaired respiration, and eventual microbial cell death.[51]

In Valence Band

$$e^- + h^+ \rightarrow ZnO + H_2O \rightarrow H^+ + OH^- \quad (3)$$

In Conduction Band

$$O_2 + e^- \rightarrow O_2\bullet^- \quad (4)$$

$$O_2\bullet^- + H^+ \rightarrow HO_2\bullet \quad (5)$$

$$HO_2\bullet + e^- \rightarrow H_2O^- \quad (6)$$

$$H_2O^- + H^+ \rightarrow H_2O_2 \quad (7)$$

Collectively, these findings underscore the synergistic antimicrobial action of ZnO NPs, which combines ionic interactions, enzymatic interference, mechanical disruption, and oxidative stress. The green synthesis approach employed in the present study offers a promising and environmentally benign platform for producing ZnO NPs with potent and broad-spectrum antimicrobial properties.[52]

Collectively, these findings underscore the synergistic antimicrobial action of ZnO NPs, which combines ionic interactions, enzymatic interference, mechanical disruption, and oxidative stress. The green synthesis approach employed in the present study offers a promising and environmentally benign platform for producing ZnO NPs with potent and broad-spectrum antimicrobial properties.[52]

The antimicrobial potential of the biosynthesized ZnO NPs was further validated through Minimum Inhibitory Concentration (MIC) assays, which provided quantitative insight into their efficacy against clinically relevant pathogens. The MIC values determined for Pseudomonas aeruginosa, methicillin-resistant Staphylococcus aureus (MRSA), and Candida species were 550 µg/mL, 630 µg/mL, and 325 µg/mL, respectively. These concentrations represent the lowest amounts of ZnO NPs required to achieve complete inhibition of microbial growth under the test conditions.[53,54]

The comparatively lower MIC observed for Candida species highlights the susceptibility of fungal cells to ZnO NPs, possibly due to the interaction of Zn^{2+} ions with structural polysaccharides and membrane-bound proteins. In contrast, the slightly higher MIC values required for bacterial strains may be attributed to differences in cell wall architecture and resistance mechanisms between gram-negative and gram-positive bacteria.

Overall, the MIC results substantiate the broad-spectrum antimicrobial activity of the green-synthesized ZnO NPs. Their effectiveness at relatively low concentrations, particularly against fungal pathogens, suggests their practical applicability in biomedical formulations aimed at controlling resistant and opportunistic infections.[55]

3.6 Biofilm inhibition assays

3.6.1 Assessment of biofilm biomass

ZnO NPs demonstrated significant antibiofilm activity, exhibiting inhibition rates of approximately 35%, 55%, and 63% against Pseudomonas aeruginosa, methicillin-resistant Staphylococcus aureus (MRSA), and Candida species, respectively, as shown in Fig. 5. These findings indicate that ZnO NPs are effective in disrupting both bacterial and fungal biofilm . Treatment with ZnO NPs resulted in the disruption of intracellular components in P. aeruginosa, highlighting their strong antimicrobial properties.[56] The study also revealed that increasing concentrations of ZnO NPs enhanced the degradation of biofilm-forming adherent cells, confirming a concentration-dependent antibiofilm effect. Even at low concentrations, biosynthesized ZnO NPs showed considerable antibacterial activity, with complete inhibition of multidrug-resistant pathogens observed at the lowest concentration tested.[57] These results suggest that ZnO NPs possess broad-spectrum potential as an effective antimicrobial and

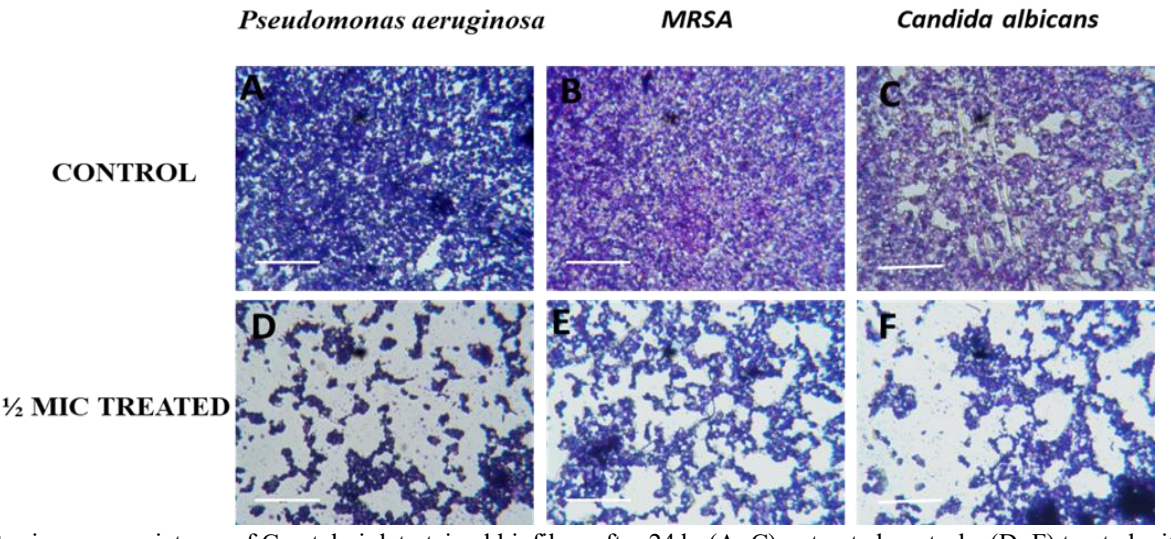


Fig. 5: Light microscopy pictures of Crystal violet-stained biofilms after 24 h: (A–C) untreated controls; (D–F) treated with ½ MIC of ZnO NPs. Images captured at 100 µm magnification.

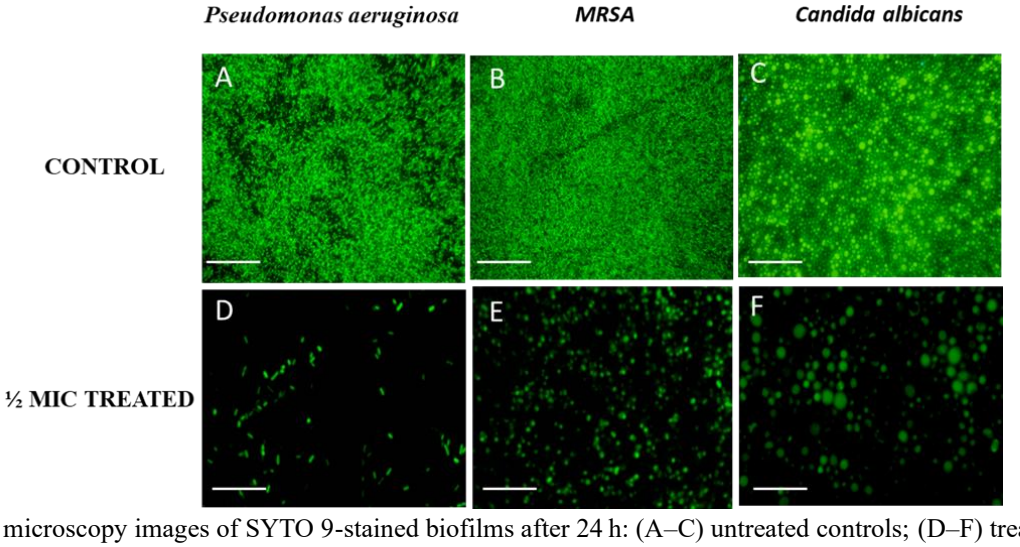


Fig. 6: Fluorescent microscopy images of SYTO 9-stained biofilms after 24 h: (A–C) untreated controls; (D–F) treated with ½ MIC of ZnO NPs. Images captured at 100 µm magnification.

antibiofilm agent.

3.6.2 Fluorescent imaging analysis

Fluorescence imaging revealed that untreated biofilms formed compact, multi-layered structures that were firmly adhered to the surface. In contrast, biofilms treated with ZnO NPs (ZnO NPs) appeared disrupted, with reduced thickness and poor surface attachment. The treated samples showed scattered, loosely arranged cell clusters, indicating weakened biofilm integrity (Fig. 6). Using SYTO 9 staining, strong green fluorescence was observed in the control group, representing viable cells within the biofilm. However, ZnO NP treatment at ½ MIC concentration significantly reduced fluorescence intensity in P. aeruginosa, MRSA, and Candida albicans. This decrease in fluorescence confirmed the notable anti-biofilm activity of ZnO NPs.[58]

3.7 Evaluation of in vitro antioxidant property

The antioxidant potential of the green-synthesized ZnO NPs (ZnO NPs) was assessed using the DPPH (2,2-diphenyl-1-picrylhydrazyl) free radical scavenging assay, a well-established method for evaluating radical-scavenging activity. The DPPH scavenging effect (% inhibition) was calculated using Eq. (8).The notable antioxidant performance of the ZnO NPs can be attributed to the presence of surface-bound phytochemicals from the *A. officinarum* extract, which serve as capping and stabilizing agents. These bioactive compounds, rich in hydroxyl and phenolic groups, effectively donate hydrogen atoms or electrons to neutralize free radicals.

The nanoscale dimensions and high surface area of ZnO NPs further enhance their reactivity, promoting stronger interaction with DPPH radicals. The mechanism involves the reduction of the deep violet DPPH radical, which shows maximum absorbance at 517 nm. Upon interaction with an antioxidant, this absorbance diminishes and shifts toward yellow, indicating successful free radical scavenging.[59,60]

$$DPPH\ scavenging\ effect\ (\%\ inhibition) = \frac{Absorbance\ of\ control - Absorbance\ of\ reaction}{Absorbance\ of\ control} \times 100 \quad (8)$$

The antioxidant activity of the biosynthesized ZnO NPs was evaluated at various concentrations. The percentage of inhibition observed for ZnO NPs ranged from 39.21% at 10 µg/mL to 68.23% at 500 µg/mL, demonstrating a concentration-dependent increase in radical scavenging activity (Table 2).

Table 2: DPPH assay values (percentage of inhibition) of ZnO NPs.

SI.NO	Treated sample concentration(µg/ml)	Percentage of inhibition(%)
1	Ascorbic acid	91.21
2	500 µg/ml	68.23
3	250 µg/ml	56.17
4	100 µg/ml	48.32
5	50 µg/ml	41.17
6	10 µg/ml	39.21

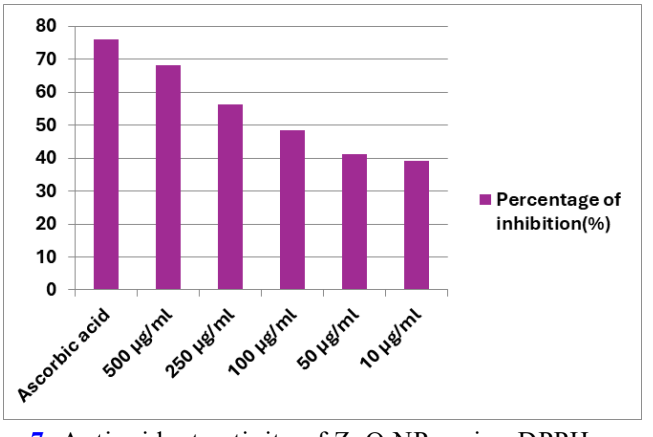


Fig. 7: Antioxidant activity of ZnO NPs using DPPH assay.

Although the antioxidant activity of the green-synthesized ZnO NPs was comparatively lower than that of the standard antioxidant, ascorbic acid (which exhibited 91.21% inhibition), the results presented in Fig. 7 demonstrate the notable free radical scavenging potential of the nanoparticles.[61] The ZnO NPs achieved a maximum inhibition of 68.23% at 500 µg/mL, with an IC_{50} value of 245 µg/mL, indicating moderate but effective antioxidant capacity. These findings support the potential of green-synthesized ZnO NPs as viable agents for mitigating oxidative stress, with relevance to various biomedical and therapeutic applications.

4. Conclusion

ZnO NPs were synthesized by a green and sustainable method employing *A. officinarum* rhizome extract as a bioreducing and stabilizing agent. The structural properties of the synthesized ZnO NPs were confirmed by X-ray diffraction (XRD), which revealed a hexagonal wurtzite crystalline phase with an average crystallite size of approximately 20 nm. Fourier-transform infrared spectroscopy (FT-IR) indicated the presence of functional moieties derived from the plant extract, suggesting their involvement in nanoparticle stabilization. TEM analysis revealed that the synthesized ZnO NPs were predominantly spherical, with an average diameter of 26 nm. The SAED patterns exhibited intense reflections corresponding to the lattice plane (101) with high intensity, 36.25 ° as d-spacing value, which well matched with XRD results.

The biosynthesized ZnO NPs displayed notable antimicrobial activity against both Gram-positive and Gram-negative bacterial strains, underscoring their potential as antimicrobial agents, particularly in the context of multidrug-resistant pathogens. In addition, the nanoparticles exhibited significant anti-biofilm activity, which is of particular relevance in the treatment of biofilm-associated infections that are resistant to conventional antibiotics. Antioxidant assays further demonstrated the nanoparticles' efficacy in scavenging free radicals, highlighting their potential application in biomedical fields such as wound healing, drug delivery, and medical textiles.

Although the biological activity of ZnO NPs is known to be dose-dependent and higher concentrations may raise toxicity concerns, the use of a green synthesis route offers advantages in terms of safety and environmental sustainability. Future research will aim to evaluate the anticancer activity of these nanoparticles, with particular focus on their effects against the MCF-7 human breast cancer cell line, to further explore their therapeutic potential. This study contributes to the growing body of literature on plant-mediated synthesis of nanomaterials and their multifunctional applications in biomedical sciences.

Acknowledgments

The authors would like to thank the basic support from the National Institute of Technology, Puducherry, Karaikal, India. The authors gratefully acknowledge Central Instrumentation Facility (CIF), Pondicherry University for extending their instrumentation facilities.

Conflict of Interest

The authors declare that there is no conflict of in terest.

Nomenclature

ZnO: Zinc oxide
NPs: Nanoparticles
MIC: Minimum Inhibitory Concentration
MHB: Mueller Hinton Broth
DPPH: 2,2-diphenyl-1-picrylhydrazyl
XRD: X-ray Diffraction
FTIR: Fourier Transform Infrared Spectroscopy
TEM: Transmission Electron Microscope

Supporting Information

Not applicable.

CRediT Statement

Nishkala Krishnamoorthy: Conceptualization, Methodology, Experimental investigation (green synthesis, characterization, and biological evaluation of ZnO nanoparticles), Data curation and Writing - Original draft preparation. **Suganya Kannan:** Validation, Formal analysis, Visualization and Writing - Review & editing. **Ragupathy Dhanusuraman:** Supervision, Resources, Project administration, Funding acquisition and Writing - Review & editing.

References

[1] I. Khan, K. Saeed, I. Khan, Nanoparticles: properties, applications and toxicities, *Arabian Journal of Chemistry*, 2019, **12**, 908-931, doi: 10.1016/j.arabjc.2017.05.011.

[2] V. S. Sivasankarapillai, N. Krishnamoorthy, G. E. Eldesoky, S. M. Wabaidur, M. A. Islam, R. Dhanusuraman, V. K. Ponnusamy, One-pot green synthesis of ZnO nanoparticles using Scoparia Dulcis plant extract for antimicrobial and antioxidant activities, *Applied Nanoscience*, 2023, **13**, 6093-6103, doi: 10.1007/s13204-022-02610-7.

[3] S. A. Akintelu, A. S. Folorunso, A review on green synthesis of zinc oxide nanoparticles using plant extracts and its biomedical applications, *BioNanoScience*, 2020, **10**, 848-863, doi: 10.1007/s12668-020-00774-6.

[4] J. C. Diel, D. S. P. Franco, A. V. Igansi, T. R. S. Cadaval, H. A. Pereira, I. dos S. Nunes, C. W. Basso, M. do Carmo M. Alves, J. Morais, D. Pinto, G. L. Dotto, Green synthesis of carbon nanotubes impregnated with metallic nanoparticles: Characterization and application in glyphosate adsorption, *Chemosphere*, 2021, **283**, 131193, doi: 10.1016/j.chemosphere.2021.131193.

[5] M. Zeraati, V. Alizadeh, S. Chupradit, N. P. S. Chauhan, G. Sargazi, Green synthesis and mechanism analysis of a new metal-organic framework constructed from Al (III) and 3, 4-dihydroxycinnamic acid extracted from Satureja hortensis and its anticancerous activities, *Journal of Molecular Structure*, 2022, **1250**, 131712, doi: 10.1016/j.molstruc.2021.131712.

[6] C. Abinaya, R. Manjula Devi, P. Suresh, N. Balasubramanian, N. Muthaiya, N. D. Kannan, J. Annaraj, V. Shanmugaiah, J. M. Pearce, P. Shanmugapriya, J. Mayandi, Antibacterial and anticancer activity of hydrothermally-synthesized zinc oxide nanomaterials using natural extracts of neem, pepper and turmeric as solvent media, *Nano Express*, 2020, **1**, 010029, doi: 10.1088/2632-959X/ab8a76.

[7] A. Kołodziejczak-Radzimska, T. Jesionowski, Zinc oxide: from synthesis to application: a review, *Materials*, 2014, **7**, 2833-2881, doi: 10.3390/ma7042833.

[8] A. C. Dhanemozhi, V. Rajeswari, S. Sathyajothi, Green synthesis of zinc oxide nanoparticle using green tea leaf extract for supercapacitor application, *Materials Today: Proceedings*, 2017, **4**, 660-667, doi: 10.1016/j.matpr.2017.01.070.

[9] S. Fakhari, M. Jamzad, H. Kabiri Fard, Green synthesis of zinc oxide nanoparticles: a comparison, *Green Chemistry Letters and Reviews*, 2019, **12**, 19-24, doi: 10.1080/17518253.2018.1547925.

[10] N. Krishnamoorthy, V. S. Sivasankarapillai, V. K. Natarajan, G. E. Eldesoky, S. M. Wabaidur, M. Eswaran, R. Dhanusuraman, Biocidal activity of ZnO NPs against pathogens and antioxidant activity - a greener approach by Citrus hystrix leaf extract as bio-reductant, *Biochemical Engineering Journal*, 2023, **192**, 108818, doi: 10.1016/j.bej.2023.108818.

[11] J. A. A. Abdullah, M. J. Rosado, A. Guerrero, A. Romero, Eco-friendly synthesis of ZnO-nanoparticles using *Phoenix dactylifera* L., polyphenols: physicochemical, microstructural, and functional assessment, *New Journal of Chemistry*, 2023, **47**, 4409-4417, doi: 10.1039/D3NJ00131H.

[12] P. Singh, Y.-J. Kim, D. Zhang, D.-C. Yang, Biological synthesis of nanoparticles from plants and microorganisms, *Trends in Biotechnology*, 2016, **34**, 588-599, doi: 10.1016/j.tibtech.2016.02.006.

[13] C. Ashajyothi, K. H. Harish, N. Dubey, R. K. Chandrakanth, Antibiofilm activity of biogenic copper and zinc oxide nanoparticles-antimicrobials collegiate against multiple drug resistant bacteria: a nanoscale approach, *Journal of Nanostructure in Chemistry*, 2016, **6**, 329-341, doi: 10.1007/s40097-016-0205-2.

[14] A. K. Ramanunny, S. Wadhwa, M. Gulati, S. Vishwas, R. Khursheed, K. R. Paudel, S. Gupta, O. Porwal, S. M. Alshahrani, N. K. Jha, D. K. Chellappan, P. Prasher, G. Gupta, J. Adams, K. Dua, D. Tewari, S. K. Singh, Journey of Alpinia galanga from kitchen spice to nutraceutical to folk medicine to nanomedicine, *Journal of Ethnopharmacology*, 2022, **291**, 115144, doi: 10.1016/j.jep.2022.115144.

[15] L. P. Köse, İ. Gülçin, A. C. Gören, J. Na miesnik, A. L. Martinez-Ayala, S. Gorinstein, LC–MS/MS analysis, antioxidant and anticholinergic properties of galanga (Alpinia officinarum Hance) rhizomes, *Industrial Crops and Products*, 2015, **74**, 712-721, doi: 10.1016/j.indcrop.2015.05.034.

[16] V. S. Honmore, A. D. Kandhare, P. P. Kadam, V. M. Khedkar, D. Sarkar, S. L. Bodhankar, A. A. Zanwar, S. R. Rojatkar, A. D. Natu, Isolates of alpinia officinarum hance as COX-2 inhibitors: evidence from anti-inflammatory, antioxidant and molecular docking studies, *International Immunopharmacology*, 2016, **33**, 8-17, doi: 10.1016/j.intimp.2016.01.024.

[17] A. R. Srividya, S. P. Dhanabal, V. K. Misra, G. Suja, Antioxidant and antimicrobial activity of*alpinia officinarum*, *Indian Journal of Pharmaceutical Sciences*, 2010, **72**, 145, doi: 10.4103/0250-474x.62233.

[18] D. Shin, K. Kinoshita, K. Koyama, K. Takahashi, Antiemetic principles of *Alpinia officinarum*, *Journal of Natural Products*, 2002, **65**, 1315-1318, doi: 10.1021/np020099i.

[19] N. An, Z.-M. Zou, Z. Tian, X.-Z. Luo, S.-L. Yang, L.-Z. Xu, Diarylheptanoids from the rhizomes of *Alpinia officinarum* and their anticancer activity, *Fitoterapia*, 2008, **79**, 27-31, doi: 10.1016/j.fitote.2007.07.001.

[20] H. Matsuda, S. Nakashima, Y. Oda, S. Nakamura, M. Yoshikawa, Melanogenesis inhibitors from the rhizomes of *Alpinia officinarum* in B16 melanoma cells, *Bioorganic & Medicinal Chemistry*, 2009, **17**, 6048-6053, doi: 10.1016/j.bmc.2009.06.057.

[21] Z. Zhang, G. Xin, G. Zhou, Q. Li, V. P. Veeraraghavan, S. Krishna Mohan, D. Wang, F. Liu, Green synthesis of silver nanoparticles from *Alpinia officinarum* mitigates cisplatin-induced nephrotoxicity *via* down-regulating apoptotic pathway in rats, *Artificial Cells, Nanomedicine, and Biotechnology*, 2019, **47**, 3212-3221, doi: 10.1080/21691401.2019.1645158.

[22] C. Hu, W. Zhu, Y. Lu, Y. Ren, J. Gu, Y. Song, J. He, *Alpinia*

officinarum mediated copper oxide nanoparticles: synthesis and its antifungal activity against Colletotrichum gloeosporioides, *Environmental Science and Pollution Research*, 2023, **30**, 28818-28829, doi: 10.1007/s11356-022-24225-9.
[23] J.-J. Lee, J.-H. Lee, N.-H. Yim, J.-H. Han, J. Y. Ma, Application of galangin, an active component of *Alpinia officinarum* Hance (Zingiberaceae), for use in drug-eluting stents, *Scientific Reports*, 2017, **7**, 8207, doi: 10.1038/s41598-017-08410-2.
[24] P. Bhattacharyya, B. Agarwal, M. Goswami, D. Maiti, S. Baruah, P. Tribedi, Zinc oxide nanoparticle inhibits the biofilm formation of Streptococcus pneumoniae, *Antonie Van Leeuwenhoek*, 2018, **111**, 89-99, doi: 10.1007/s10482-017-0930-7.
[25] F. B. dos Reis-Teixeira, V. F. Alves, E. C. P. de Martinis, Growth, viability and architecture of biofilms of Listeria monocytogenes formed on abiotic surfaces, *Brazilian Journal of Microbiology*, 2017, **48**, 587-591, doi: 10.1016/j.bjm.2017.01.004.
[26] A. Braca, N. De Tommasi, L. Di Bari, C. Pizza, M. Politi, I. Morelli, Antioxidant principles from *Bauhinia tarapotensis*, *Journal of Natural Products*, 2001, **64**, 892-895, doi: 10.1021/np0100845.
[27] W.-X. Zhang, I.-C. Chao, D.-J. Hu, F. Shakerian, L. Ge, X. Liang, Y. Wang, J. Zhao, S.-P. Li, Comparison of antioxidant activity and main active compounds among different parts of *Alpinia officinarum* hance using high-performance thin layer chromatography-bioautography, *Journal of AOAC International*, 2019, **102**, 726-733, doi: 10.5740/jaoacint.18-0307.
[28] V. Balamurugan, S. Velurajan, & A. Palanisamy, Phytochemical analysis of Alpinia officinarum and to test its Anti-oxidant, Anti-microbial, Anti-inflammatory and Antiarthritic activity, *International Journal of Advance Research And Innovative Ideas In Education*, 2019, **5**(4), 1125-1140.26-733.
[29] Y. Y. Chan, Y. L. Pang, S. Lim, W. C. Chong, Facile green synthesis of ZnO nanoparticles using natural-based materials: Properties, mechanism, surface modification and application, *Journal of Environmental Chemical Engineering*, 2021, **9**, 105417, doi: 10.1016/j.jece.2021.105417.
[30] V. S. Sivasankarapillai, A. Sundararajan, M. Eswaran, R. Dhanusuraman, Hierarchical activated porous activated carbon derived from callistemon leaf biochar for supercapacitor and methylene blue removal applications, *ES Energy & Environment*, 2024, **24**, doi: 10.30919/esee1124.
[31] A. Happy, M. Soumya, S. Venkat Kumar, S. Rajeshkumar, R. D. Sheba, T. Lakshmi, V. Deepak Nallaswamy, Phyto-assisted synthesis of zinc oxide nanoparticles using Cassia alata and its antibacterial activity against Escherichia coli, *Biochemistry and Biophysics Reports*, 2019, **17**, 208-211, doi: 10.1016/j.bbrep.2019.01.002.
[32] R. Yuvakkumar, J. Suresh, B. Saravanakumar, A. Joseph Nathanael, S. I. Hong, V. Rajendran, Rambutan peels promoted biomimetic synthesis of bioinspired zinc oxide nanochains for biomedical applications, *Spectrochimica Acta Part A: Molecular and Biomolecular Spectroscopy*, 2015, **137**, 250-258, doi: 10.1016/j.saa.2014.08.022.
[33] K. Vimala, S. Sundarraj, M. Paulpandi, S. Vengatesan, S. Kannan, Green synthesized doxorubicin loaded zinc oxide nanoparticles regulates the Bax and Bcl-2 expression in breast and colon carcinoma, *Process Biochemistry*, 2014, **49**, 160-172, doi: 10.1016/j.procbio.2013.10.007.
[34] J. Osuntokun, D. C. Onwudiwe, E. E. Ebenso, Green synthesis of ZnO nanoparticles using aqueous *Brassica oleracea* L. var. *italica* and the photocatalytic activity, *Green Chemistry Letters and Reviews*, 2019, **12**, 444-457, doi: 10.1080/17518253.2019.1687761.
[35] S. Ş. Doğan, A. Kocabaş, Green synthesis of ZnO nanoparticles with *Veronica multifida* and their antibiofilm activity, *Human & Experimental Toxicology*, 2020, **39**, 319-327, doi: 10.1177/0960327119888270.
[36] S. S. Momeni, M. Nasrollahzadeh, A. Rustaiyan, Green synthesis of the Cu/ZnO nanoparticles mediated by Euphorbia prolifera leaf extract and investigation of their catalytic activity, *Journal of Colloid and Interface Science*, 2016, **472**, 173-179, doi: 10.1016/j.jcis.2016.03.042.
[37] M. Arumugam, B. Murugesan, N. Pandiyan, D. K. Chinnalagu, G. Rangasamy, S. Mahalingam, Electrospinning cellulose acetate/silk fibroin/Au-Ag hybrid composite nanofiber for enhanced biocidal activity against MCF-7 breast cancer cell, *Materials Science and Engineering: C*, 2021, **123**, 112019, doi: 10.1016/j.msec.2021.112019.
[38] A. J. Kulandaisamy, J. R. Reddy, P. Srinivasan, K. J. Babu, G. K. Mani, P. Shankar, J. B. B. Rayappan, Room temperature ammonia sensing properties of ZnO thin films grown by spray pyrolysis: Effect of Mg doping, *Journal of Alloys and Compounds*, 2016, **688**, 422-429, doi: 10.1016/j.jallcom.2016.07.050.
[39] M. Khatamian, Z. Alaji, A. A. Khandar, Synthesis and characterization of polycrystalline ZnO/HZSM-5 nanocomposites, *Journal of the Iranian Chemical Society*, 2011, **8**, S44-S54, doi: 10.1007/BF03254281.
[40] S.-H. Yi, S.-K. Choi, J.-M. Jang, J.-A. Kim, W.-G. Jung, Low-temperature growth of ZnO nanorods by chemical bath deposition, *Journal of Colloid and Interface Science*, 2007, **313**, 705-710, doi: 10.1016/j.jcis.2007.05.006.
[41] V. Dincă, A. Mocanu, G. Isopencu, C. Busuioc, S. Brajnicov, A. Vlad, M. Icriverzi, A. Roseanu, M. Dinescu, M. Stroescu, A. Stoica-Guzun, M. Suchea, Biocompatible pure ZnO nanoparticles-3D bacterial cellulose biointerfaces with antibacterial properties, *Arabian Journal of Chemistry*, 2020, **13**, 3521-3533, doi: 10.1016/j.arabjc.2018.12.003.
[42] A. C. Janaki, E. Sailatha, S. Gunasekaran, Synthesis, characteristics and antimicrobial activity of ZnO nanoparticles, *Spectrochimica Acta Part A: Molecular and Biomolecular Spectroscopy*, 2015, **144**, 17-22, doi: 10.1016/j.saa.2015.02.041.
[43] R. Dobrucka, J. Długaszewska, Biosynthesis and antibacterial activity of ZnO nanoparticles using Trifolium pratense flower extract, *Saudi Journal of Biological Sciences*, 2016, **23**, 517-523, doi: 10.1016/j.sjbs.2015.05.016.
[44] M. M. Chikkanna, S. E. Neelagund, K. K. Rajashekarappa, Green synthesis of Zinc oxide nanoparticles (ZnO NPs) and their biological activity, *SN Applied Sciences*, 2018, **1**, 117, doi: 10.1007/s42452-018-0095-7.
[45] J. Jayabalan, G. Mani, N. Krishnan, J. Pernabas, J. M. Devadoss, H. T. Jang, Green biogenic synthesis of zinc oxide nanoparticles using Pseudomonas putida culture and its *in vitro* antibacterial and anti-biofilm activity, *Biocatalysis and Agricultural Biotechnology*, 2019, **21**, 101327, doi: 10.1016/j.bcab.2019.101327.
[46] M. Ahamad Khan, S. Ahmad Lone, M. Shahid, M. T. Zeyad, A. Syed, A. Ehtram, A. M. Elgorban, M. Verma, M. Danish,

Phytogenically synthesized zinc oxide nanoparticles (ZnO-NPs) potentially inhibit the bacterial pathogens: in vitro studies, *Toxics*, 2023, **11**, 452, doi: 10.3390/toxics11050452.
[47] N. Sharma, J. Kumar, S. Thakur, S. Sharma, V. Shrivastava, Antibacterial study of silver doped zinc oxide nanoparticles against Staphylococcus aureus and Bacillus subtilis, *Drug Invention Today*, 2013, **5**, 50-54, doi: 10.1016/j.dit.2013.03.007.
[48] X. Zhang, H. Tang, M. Xue, C. Li, Facile synthesis and characterization of ultrathin MoS_2 nanosheets, *Materials Letters*, 2014, **130**, 83-86, doi: 10.1016/j.matlet.2014.05.078.
[49] H. Shah, Manikandan, B. Ahmed M, V. Ganesan, Enhanced bioactivity of Ag/ZnO nanorods-a comparative antibacterial study (sbds), *Journal of Nanomedicine & Nanotechnology*, 2017, **4**(3), 1000168, doi: 10.4172/2157-7439.1000168.
[50] L.-Q. Fan, G.-J. Liu, C.-Y. Zhang, J.-H. Wu, Y.-L. Wei, Facile one-step hydrothermal preparation of molybdenum disulfide/carbon composite for use in supercapacitor, *International Journal of Hydrogen Energy*, 2015, **40**, 10150-10157, doi: 10.1016/j.ijhydene.2015.06.061.
[51] X. Yang, H. Shao, W. Liu, W. Gu, X. Shu, Y. Mo, X. Chen, Q. Zhang, M. Jiang, Endoplasmic reticulum stress and oxidative stress are involved in ZnO nanoparticle-induced hepatotoxicity, *Toxicology Letters*, 2015, **234**, 40-49, doi: 10.1016/j.toxlet.2015.02.004.
[52] V. K. Bhatt, M. Patel, P. M. Pataniya, B. D. Iyer, C. K. Sumesh, D. J. Late, Enhanced antifungal activity of WS_2/ZnO nanohybrid against Candida albicans, *ACS Biomaterials Science & Engineering*, 2020, **6**, 6069-6075, doi: 10.1021/acsbiomaterials.0c00786.
[53] G. D. Amita, S. Singh, R. Singh, A. Chauhan and M.L Aggarwal, In vitro antimicrobial activity of Lemon grass oil by MIC and agar well diffusion method, *Universities' Journal of Phytochemistry and Ayurvedic Heights*, 2020, **1**, 80-86, doi: 10.51129/ujpah-2020-28-1-12.
[54] R. K. Sharma, R. Ghose, Synthesis of zinc oxide nanoparticles by homogeneous precipitation method and its application in antifungal activity against Candida albicans, *Ceramics International*, 2015, **41**, 967-975, doi: 10.1016/j.ceramint.2014.09.016.
[55] M. O'Shaughnessy, P. McCarron, L. Viganor, M. McCann, M. Devereux, O. Howe, The antibacterial and anti-biofilm activity of metal complexes incorporating 3, 6, 9-trioxaundecanedioate and 1, 10-phenanthroline ligands in clinical isolates of *Pseudomonas aeruginosa* from Irish cystic fibrosis patients, *Antibiotics*, 2020, **9**, 674, doi: 10.3390/antibiotics9100674.
[56] M. A. Reyes-Torres, E. Mendoza-Mendoza, Á. M. Miranda-Hernández, M. A. Pérez-Díaz, M. López-Carrizales, R. D. Peralta-Rodríguez, R. Sánchez-Sánchez, F. Martinez-Gutierrez, Synthesis of CuO and ZnO nanoparticles by a novel green route: Antimicrobial activity, cytotoxic effects and their synergism with ampicillin, *Ceramics International*, 2019, **45**, 24461-24468, doi: 10.1016/j.ceramint.2019.08.171.
[57] M. Maruthupandy, G. Rajivgandhi, T. Muneeswaran, J.-M. Song, N. Manoharan, Biologically synthesized zinc oxide nanoparticles as nanoantibiotics against ESBLs producing gram negative bacteria, *Microbial Pathogenesis*, 2018, **121**, 224-231, doi: 10.1016/j.micpath.2018.05.041.
[58] F. M. Husain, F. A. Qais, I. Ahmad, M. J. Hakeem, M. H. Baig, J. Masood Khan, N. A. Al-Shabib, Biosynthesized zinc oxide nanoparticles disrupt established biofilms of pathogenic bacteria, *Applied Sciences*, 2022, **12**, 710, doi: 10.3390/app12020710.
[59] H. Ashraf, B. Meer, J. Iqbal, J. S. Ali, A. Andleeb, H. Butt, M. Zia, A. Mehmood, M. Nadeem, S. Drouet, J.-P. Blondeau, N. Giglioli-Guivarc'h, C. Liu, C. Hano, B. H. Abbasi, Comparative evaluation of chemically and green synthesized zinc oxide nanoparticles: their *in vitro* antioxidant, antimicrobial, cytotoxic and anticancer potential towards HepG2 cell line, *Journal of Nanostructure in Chemistry*, 2023, **13**, 243-261, doi: 10.1007/s40097-021-00460-3.
[60] S. Khorrami, A. Zarepour, A. Zarrabi, Green synthesis of silver nanoparticles at low temperature in a fast pace with unique DPPH radical scavenging and selective cytotoxicity against MCF-7 and BT-20 tumor cell lines, *Biotechnology Reports*, 2019, **24**, e00393, doi: 10.1016/j.btre.2019.e00393.
[61] A. A. Alyamani, S. Albukhaty, S. Aloufi, F. A. AlMalki, H. Al-Karagoly, G. M. Sulaiman, Green fabrication of zinc oxide nanoparticles using *Phlomis* leaf extract: characterization and in vitro evaluation of cytotoxicity and antibacterial properties, *Molecules*, 2021, **26**, 6140, doi: 10.3390/molecules26206140.

Publisher's Note: Engineered Science Publisher remains neutral with regard to jurisdictional claims in published maps and institutional affiliations.

Open Access
This article is licensed under a Creative Commons Attribution-NonCommercial-NoDerivatives 4.0 International, which permits the use, sharing, adaptation, distribution and reproduction in any medium or format, as long as appropriate credit to the original author(s) and the source is given by providing a link to the Creative Commons license. This usage for commercial purposes is not allowed. If modifications, adaptations or any other transformation were made, it is not allowed for distribution. The images or other third-party material in this article are included in the article's Creative Commons license, unless indicated otherwise in a credit line to the material. If material is not included in the article's Creative Commons license and your intended use is not permitted by statutory regulation or exceeds the permitted use, you will need to obtain permission directly from the copyright holder. To view a copy of this license, visit https://creativecommons.org/licenses/by-nc-nd/4.0/.

©The Author(s) 2025.